



**HAL**  
open science

# Permeability and damage of partially saturated concrete exposed to elevated temperature

Hognon Sogbossi, Jérôme Verdier, Stéphane Multon

## ► To cite this version:

Hognon Sogbossi, Jérôme Verdier, Stéphane Multon. Permeability and damage of partially saturated concrete exposed to elevated temperature. *Cement and Concrete Composites*, 2020, 109, pp.103563. 10.1016/j.cemconcomp.2020.103563 . hal-02617082

**HAL Id: hal-02617082**

**<https://insa-toulouse.hal.science/hal-02617082v1>**

Submitted on 27 Sep 2023

**HAL** is a multi-disciplinary open access archive for the deposit and dissemination of scientific research documents, whether they are published or not. The documents may come from teaching and research institutions in France or abroad, or from public or private research centers.

L'archive ouverte pluridisciplinaire **HAL**, est destinée au dépôt et à la diffusion de documents scientifiques de niveau recherche, publiés ou non, émanant des établissements d'enseignement et de recherche français ou étrangers, des laboratoires publics ou privés.

1                   **Permeability and damage of partially saturated concrete exposed to**  
2   **elevated temperature**

3  
4   Hognon Sogbossi, Jérôme Verdier, Stéphane Multon\*

5                   LMDC, Université de Toulouse, INSA, UPS, 135 Avenue de Rangueil, 31077 Toulouse  
6   cedex 04, France

---

7  
8  
9                   **Abstract**

10                   This work analyses the impact of elevated temperature on the permeability and on the damage  
11                   of concrete according to its saturation degree. The Young Modulus and gas permeability were  
12                   measured on samples with different initial saturation degrees that were subjected to thermal  
13                   loading (80, 150 and 200 °C). These conditions were defined to simulate the hydrothermal  
14                   loading of nuclear plant concrete in case of accident. To analyse the behaviour of concrete  
15                   exposed to high temperature, it is necessary to distinguish the effects of water saturation and  
16                   the impact of damage on permeability. Experimentations shows that concrete with high  
17                   saturation degree can be permeable to air after thermal loading, while it was not permeable  
18                   before the loading. Relations are proposed to link the permeability variation to temperature  
19                   according to the initial saturation degree of the concrete and to evaluate the permeability  
20                   variation from the induced damage.

21  
22  
23                   **Keywords:** *Damage; Durability; Permeability; Saturation degree; Temperature; Transport*  
24                   *Properties*

---

25  
26  
27  
28  
29                   \*Corresponding author: Email: multon@insa-toulouse.fr  
30  
31

## 32 **1 Introduction**

33 Permeability quantifies the fluid flow through a porous medium under the effect of a pressure  
34 gradient. Sealing quality of concrete is an important property for specific structures.  
35 Permeability can also be used to evaluate the durability performance of concrete.

36 Thermal loading due to temperature increase is an important risk for structures. The heating  
37 may be caused by fire or by accidental situations in nuclear power plants leading to loss of  
38 coolant accidents (LOCA). Thermal loading (increase of temperature expected from 20 °C up  
39 to 200 °C in case of LOCA) can lead to important cracking. Sealing is of prime importance for  
40 the enclosure vessels of nuclear power plants. After LOCA and resulting thermal loading, the  
41 increase of permeability due to induced thermal cracking leads to the decrease of sealing  
42 capacity. This consequence has to be evaluated to ensure the security of the equipment. The  
43 evaluation of the increase of permeability according to thermal loading is the main objective of  
44 this study.

45 Exposure to high temperature and the resulting drying lead to many evolutions in the micro and  
46 macro-structure of concrete. These evolutions have various consequences on mechanical  
47 properties [1-5] and permeability [6-12].

48 Different origins can explain the damage induced by thermal loading: physicochemical origin  
49 (decomposition of hydrates [13-16]), micromechanical origin leading to cracking (in the  
50 interfacial transition zone due to differential dilation of aggregate and cement paste [17, 18],  
51 due to drying shrinkage of paste restrained by aggregate [8], or due to the increase in vapour  
52 pressure [19, 20]) and macro mechanical origin leading to structural cracking (temperature and  
53 humidity gradient [21]). In modelling, damage during thermal loading is thus evaluated from  
54 dehydration and crack development induced by thermally induced microcracking [10, 18, 22].  
55 During drying, the reduction of the water content by evaporation due to heating [5, 23] leads  
56 also to an increase of free porosity. It has a strong impact on the connection of natural  
57 percolation paths and thus on permeability [24, 25]. The evolution of the concrete permeability  
58 after thermal loading may be regarded as a function of the accessible gas porosity due to water  
59 removal on the one hand, and as a function of diffuse micro-cracking in the material on the  
60 other [15]. The width, connectivity and tortuosity of old and newly created flow channels  
61 determine the concrete permeability after the loading.

62 Water content in concrete is adapted to obtain correct rheology during casting. As a  
63 consequence, the saturation degree of concrete is high even when cement hydration is advanced  
64 (usual concrete saturation lies between 75 and 90% for hydration degrees upper than 80%). The

65 degree of saturation of concrete stays usually high in the cores of massive structures and in  
66 locations submitted to rainfall (over 80% at 50 mm depth [26]). For lower, but current, external  
67 environmental conditions (between 50 and 60% of relative humidity), the saturation of most  
68 concrete lies also between 50 and 60%. The loss of coolant accidents (LOCA) can occur at any  
69 time of the service life of the structures. Before the accident, the saturation degree of concrete  
70 skin of the internal enclosure vessel is about 60%. The saturation degree of the core of these  
71 massive walls (about 1 meter width) can be expected between 60 and 80% [27, 28]. It is thus  
72 important to evaluate the response of the concrete exposed to elevated temperature with high  
73 initial saturation degrees.

74 The impact of temperature, saturation degree and thermal loading on concrete permeability has  
75 been widely studied and analysed in the literature [6-12, 29-35]. However, cementitious  
76 materials subjected to thermal loading in the previous experimental programs have low  
77 saturation degrees [7, 36]. The impact of exposure temperature on the permeability of partially  
78 saturated concrete has been little studied while the water saturation of porosity should have a  
79 major impact on overpressure due to thermal heating. The experimental program presented in  
80 this paper attempts to test the material under conditions close to those found in situ: the concrete  
81 is partially saturated with water at the time of the thermal loading. This gap has to be filled to  
82 be able to evaluate the containment properties after thermal loading of in situ concrete. The  
83 evolutions of the permeability and modulus of elasticity of concrete are presented and analysed.  
84 Correlation of the evolution of permeability of concrete exposed to elevated temperatures with  
85 the evolution of mechanical properties is also an important result of this study.

86

## 87 **2 Materials and methods**

### 88 **2.1 Composition of concrete mix**

89 Concrete used in this work (Table 1) is representative of a wide range of concrete used in French  
90 nuclear plants. It is the same mix that the concrete used for the Vercors mockup built by EDF  
91 to help the management of long term operation of its fleet of Nuclear Power Plants [37].  
92 Siliceous limestone aggregates were used. Silica contents of aggregates were about 80 and 5%  
93 for the sand and the gravels, respectively [38]. Twenty-four hours after casting, the samples  
94 were removed from their moulds and cured in lime water at a temperature of  $20 \pm 2$  °C for at  
95 least 60 days. This long period in lime water was required to obtain a stabilized material  
96 regarding cement hydration [39]. The mean compressive strength of the concrete was 42 MPa.

97

98 **Table 1.** Concrete mix

Constituents	[kg/m <sup>3</sup> ]
Sand 0/4	830
Gravel 4/11 R	445
Gravel 8/16 R	550
Cement CEM I 52.5 NCE CP2 NF	320
Plasticizer	2.4
Water	167

99

## 100 **2.2 Conditioning**

101 The aim of this study was to apply thermal loading to concrete with different initial saturation  
102 degrees. To control the saturation degree, the samples were exposed to drying. Such drying can  
103 generate moisture gradient, which can affect air permeability, particularly if moisture content  
104 is high. Samples underwent thus precise conditioning. This conditioning was inspired by the  
105 literature [40-42] and was intended to limit the thermo-hydric gradient and resulting skin  
106 cracking during conditioning before the tests.

107 First, the samples were fully saturated under vacuum. Then, the samples were dried in an oven  
108 with a gradually increasing drying temperature (40 °C to reach 80%, 60 °C to reach, 60%, 30  
109 and 10%, 105 °C to obtain the smallest degree of saturation assumed to be 0% in this work).  
110 The targeted masses were determined from the concrete porosity measured on other samples  
111 casted during the same concrete batch, before the conditioning of samples exposed to elevated  
112 temperatures. Once the target mass was reached, samples were packed in aluminium and sealed  
113 bags. Then, they were put back into the oven for a period of time at least equal to the drying  
114 time under watertight sealing in order to partially rehomogenize the water distribution  
115 throughout the sample and thus minimize the impact of moisture gradient on air permeability  
116 measurements [42].

117 The dry state ( $S_0 = 0\%$ ) can only be achieved with a conditioning temperature of 105 °C. Such  
118 a temperature can lead to significant cracking [43]. It is confirmed in this experimental study.  
119 The impact on the results of modulus and permeability are thus discussed in the analysis.

120

## 121 2.3 Methods

### 122 2.3.1 Modulus

123 In this work, the evolution of the concrete mechanical property is evaluated by the modulus of  
124 elasticity. It was measured on cylindrical specimens (diameter: 110 mm, height: 220 mm)  
125 according to the European standard [44]. The longitudinal deformation of the samples was  
126 measured with three gauges (KC 70 – 120- A1-11 having a gauge factor of  $2.11 \pm 1\%$ ). Gauges  
127 were stuck vertically and equidistant from one another on the lateral surface of the samples.

128 The compression test was carried out using a hydraulic cylinder mechanical press with a  
129 capacity of 4000 kN. The force was applied in autopilot mode with force control at the speed  
130 of 0.5 MPa/s, respecting the CPC8 recommendations [45], which advise testing the specimen  
131 at 30% of the breaking load over five loading/unloading cycles. The elastic modulus was  
132 calculated on the last increase in load (5<sup>th</sup> cycle) from the following relation:

$$E = \frac{\sigma_{30} - \sigma_0}{\varepsilon_{30} - \varepsilon_0} \quad \text{Eq. 1}$$

133 where  $\sigma_{30}$  is equal to 30% of the compressive strength;  $\sigma_0$  is the strain preload of the press,  
134 which is equal to 0.5 MPa;  $\varepsilon_{30}$  is the longitudinal strain corresponding to stress  $\sigma_{30}$  of the 5<sup>th</sup>  
135 cycle; and  $\varepsilon_0$  is the longitudinal strain corresponding to stress  $\sigma_0$  of the 5<sup>th</sup> cycle.

### 136 2.3.2 Permeability

137 The permeability was measured with a Cembureau permeameter. After the curing period, the  
138 samples (diameter =150 mm, h=50 mm) were sawn from the original cylindrical specimens  
139 (diameter =150 mm, h = 200 mm) and the first 20 mm of both ends were removed to avoid skin  
140 effects. The coefficient of permeability was defined by the Darcy law and the gas apparent  
141 permeability of a porous medium was calculated using the Hagen-Poiseuille relationship for  
142 laminar flow of a compressible fluid through a porous medium with small capillaries under  
143 steady-state conditions [46]:

$$k = \frac{2 \mu L}{S(P_I^2 - P_O^2)} P_a Q_O \quad \text{Eq. 2}$$

144 where  $k$  is the apparent permeability obtained for  $P_I = 2 \text{ bars}$  according to standard [47],  $P_a Q_O$   
145 is the outlet gaseous flow,  $P_I$  and  $P_O$  are inlet and outlet pressures with  $P_O$  equal to atmospheric  
146 pressure  $P_a$ ,  $S$  is the cross-sectional area of the specimen ( $\text{m}^2$ ),  $L$  is the thickness of the specimen  
147 in the direction of flow (m),  $\mu$  is the dynamic viscosity of the fluid ( $\text{N.s.m}^{-2}$ ).

## 148 **2.4 Experimental program**

### 149 *2.4.1 Impact of drying on modulus and permeability*

150 The Young modulus and the permeability of the concrete was first measured for four saturation  
151 states:  $S_w = 100\%$ ,  $60\%$ ,  $30\%$ , and  $00\%$  without thermal loading. It is necessary to quantify the  
152 effect of the drying obtained with moderate and progressive heating on the properties before  
153 the application of the thermal loading. The drying was applied to samples (diameter: 110 mm,  
154 height: 220 mm for the mechanical characterization and diameter: 150 mm, h: 50 mm for the  
155 transfer measurements) after a minimum of 60 days of curing in lime water in order to reach a  
156 stabilized material regarding hydration. The drying durations were determined according to  
157 temperature of conditioning to obtain the mass for the targeted saturation degrees as explained  
158 in the ‘conditioning’ part.

### 159 *2.4.2 Impact of thermal loading on modulus and permeability*

160 This part of the experimental program concerns the determination of the evolution of the Young  
161 modulus and of the permeability after thermal loading. The thermal loading was applied to  
162 samples (same sizes than for the study of drying) with four initial degrees of saturation (100,  
163 60, 30, and 00%) after 60 days of curing in lime water. Each sample was wrapped in aluminium  
164 and subjected to the thermal loading in an oven preheated to the target temperature  $T$ . The  
165 samples were directly exposed to the temperature in the oven. The duration of the thermal  
166 loading was 14 hours. This heating time was defined on the basis of experience gained on the  
167 slabs of the ENDE project [48]. The 14-hour duration allowed the target temperature to be  
168 reached and to be maintained for two hours in the specimen cores. The mechanical and  
169 permeability tests were performed after the return to ambient temperature. For a given  
170 temperature, three samples were tested per initial saturation degree.

171 The Young modulus was measured after thermal loading for three temperatures:  $T = 80$ , 150  
172 and  $200\text{ }^\circ\text{C}$ .

173 For the permeability measurements, twelve different samples (diam: 150 mm, h: 50 mm) were  
174 tested. The samples were first exposed to the thermal loading at  $80\text{ }^\circ\text{C}$ , then at  $150\text{ }^\circ\text{C}$  and  
175 finally at  $200\text{ }^\circ\text{C}$ . Before the exposition at  $200\text{ }^\circ\text{C}$ , the samples were resaturated to their initial  
176 saturation degree as explained just below. Permeability tests were performed between each  
177 exposure temperature and the next.

178 Samples were packed in aluminium foil to limit the loss of water during the exposure. After the  
179 thermal loading at  $80\text{ }^\circ\text{C}$ , no loss of mass was noted for any of the samples. All the water stayed

180 in the concrete during the exposure at 80 °C, and the permeability tests were performed at the  
181 initial saturation degree ( $S_{w0}$ ). After the permeability measurements, the same samples were  
182 exposed to the second thermal loading (150 °C). After the exposure at 150 °C and 200 °C,  
183 samples lost all their water content. It was decided to perform permeability tests after the return  
184 to ambient temperature for two saturation degrees:

- 185 - The first permeability test (K1) was performed directly after the thermal loading. This  
186 measurement was thus representative of dry concrete.
- 187 - The second permeability test (K2) was performed after resaturation: the permeability  
188 measurement was performed with the water content present before the temperature  
189 exposure and was representative of concrete exposed to steam and air during an accident  
190 [49, 50] and saturated again due to natural humid conditions after the accident.

191 The samples were exposed to the third thermal loading (200 °C) after the permeability test K2  
192 and thus on samples resaturated to their initial saturation degree.

193 In order to characterize the mechanisms at high saturation degree, three samples were subjected  
194 to the chosen temperature with 100% of saturation in order to simulate the case of the highest  
195 impact of water vapour. Permeability tests were then performed with 80% of saturation since  
196 there is no percolation path for gas when the material is entirely full of water (100%). At 80%  
197 of saturation, concrete permeability can be measured if the damage induced by the thermal  
198 loading is sufficient.

## 199 **3 Experimental results**

### 200 **3.1 Modulus**

#### 201 *3.1.1 Evolution with the saturation degree*

202 The evolution of the mechanical properties with the saturation degree has been well studied in  
203 the literature [1-5, 51-58]. Most of the previous studies point out an increase in strength [51-55,  
204 58] and a decrease in Young modulus [52-55, 57, 58]. In concrete submitted to drying, two  
205 main mechanisms are in competition: the strengthening of material by capillary forces and  
206 surface tension, and the damage of concrete due to micro-cracking induced by drying [1, 8, 51-  
207 53]. The first mechanism is preponderant in the strength evolution while the second mechanism  
208 has an important impact on modulus [53]. The contribution of water compressibility could also  
209 participate to greater modulus of the saturated concrete compared to dry material [58]. In some  
210 cases, a rare small increase of modulus can be observed for dry concrete [56, 59].



211 In this study, it was important to characterize the dependence of the Young modulus on the  
212 saturation degree in order to separate the impact of the temperature and the effect of the  
213 saturation degree in the following analysis. The results are in good agreement with the literature  
214 with a decrease of modulus with the saturation degree (Figure 1).

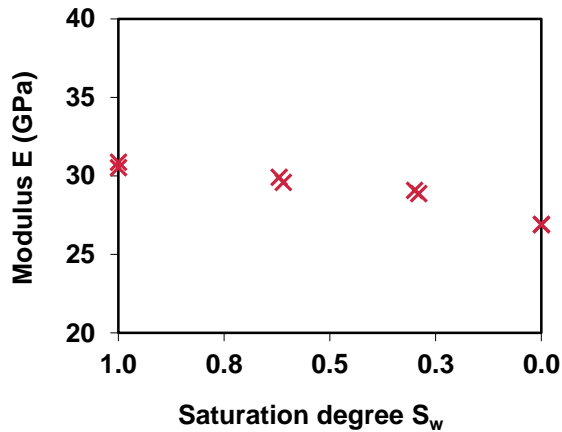


Figure 1. Evolution of modulus E as a function of the saturation degree  $S_w$

### 215 3.1.2 Evolution after thermal loading

216 The mechanical properties were measured on the concrete before and after exposure to three  
217 temperatures (80 °C, 150 °C and 200 °C) for four initial saturation states (100%, 60%, 30% and  
218 00%). The evolution of the modulus is represented as a function of temperature in Figure 2.  
219 The results of the previous part have been added ( $T = 60$  °C for samples E30, E60, E100 and  $T$   
220  $= 105$  °C for samples E00) for comparison with the three thermal loading. For a given initial  
221 degree of saturation (Figure 2), the modulus of elasticity decreases significantly with the  
222 increase in temperature, as expected from the literature.

223 The initial saturation state seems to have little impact on the evolution of the modulus. For high  
224 temperature, water vaporization occurs. For such small specimens, vapour moves out of the  
225 concrete quickly during drying and the impact of the pressure induced in the concrete is  
226 minimal. These tests were representative of concrete skin directly exposed to high temperatures  
227 or for elements with small thickness. They may not be representative of what happens in the  
228 core of a massive structure [19], although the vapour present in these areas could also migrate  
229 through the steel concrete-interfaces [60] in cases of severe thermal loads [61].

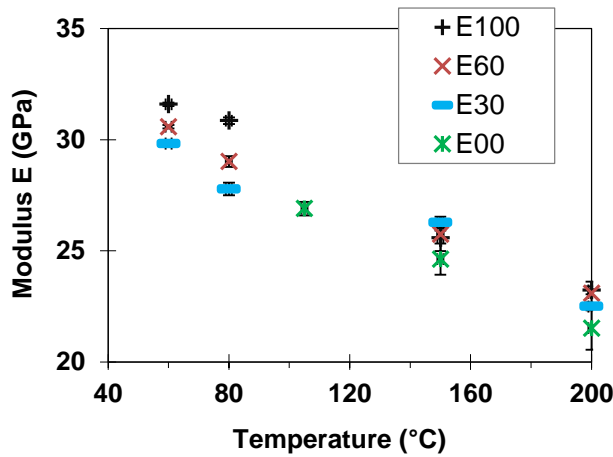


Figure 2. Evolution of the modulus  $E$  according to the temperature for four initial saturation degrees

230

### 231 3.2 Permeability

#### 232 3.2.1 Evolution with the saturation degree

233 The apparent permeability of all the samples was first tested before the thermal loading, just  
 234 after the preconditioning at 40 or 60 °C (Figure 3) in order to quantify the variation of  
 235 permeability with the saturation state. Experimental values are given in Figure 3-a versus the  
 236 saturation degree. They were used as references in the following analysis of the impact of  
 237 temperature on permeability. Even if the conditioning protocol uses moderate drying, it induces  
 238 micro-cracking, which modifies the percolation network. The increase of permeability is thus  
 239 due to the combination of the water departure and the cracking. The results are in good  
 240 agreement with previous experimental and numerical works [34, 60, 62, 63].

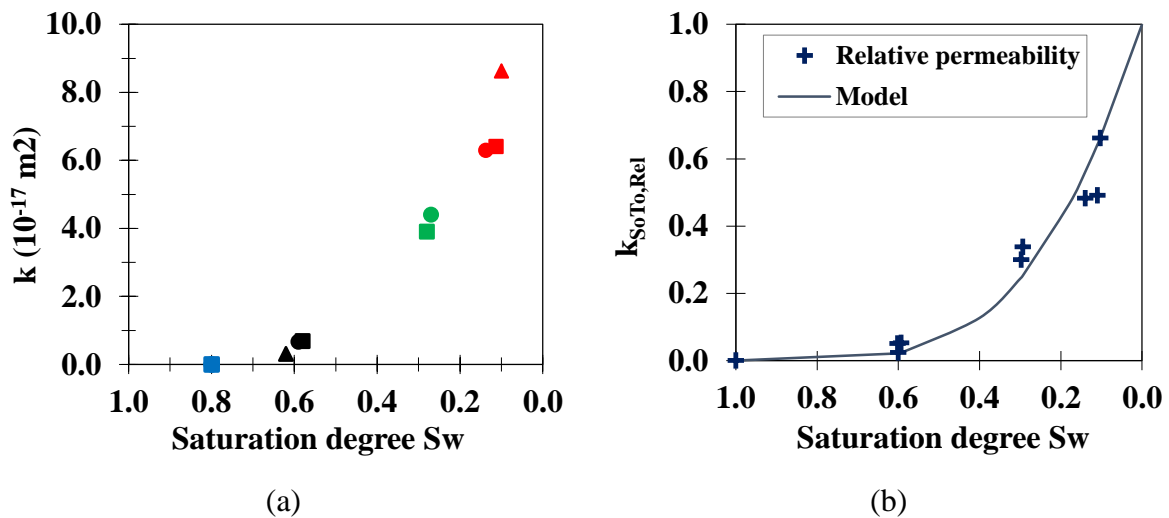


Figure 3. Evolution of apparent permeability  $k$  as a function of the saturation degree (a) and relative permeability (b)

241 Usual dispersion was observed for most samples, particularly at 10% of saturation. It can be  
 242 explained by the heterogeneity of the concrete in terms of microstructure and, more particularly,  
 243 of porosity paths accessible to gas. The heterogeneity increased with drying.

244 From these experimental results, the relative permeability was defined (Figure 3-b):

$$k_{S_0T_0-Rel} = \frac{k_{S_0}}{k_0} \quad Eq. 3$$

245 where  $k_{S_0T_0-Rel}$  is the relative permeability for the saturation degree  $S_0$ ,  $k_{S_0}$  is the apparent  
 246 permeability for the samples at the saturation degree  $S_0$  and  $k_0$  is the apparent permeability in  
 247 the dry state.

248 One of the main difficulties was to obtain the apparent permeability  $k_0$  representative of the  
 249 concrete studied. The dry state ( $S_0 = 0\%$ ) was obtained with a conditioning temperature of 105  
 250 °C. This drying leads to cracking and this state was not representative of the initial state of  
 251 concrete subjected to the thermal loading in the following experiments (exposed to less than 60  
 252 °C before the loading). To obtain relevant and representative analysis,  $k_0$  was evaluated from  
 253 the permeability measurements obtained for conditioning temperatures lower than or equal to  
 254 60 °C. A van Genuchten model [64] was used to deduce the corresponding  $k_0$  (Figure 3-b):

$$k_{S_0T_0} = k_0 \cdot \underbrace{(1 - S_w)^q (1 - S_w^{1/m})^{2m}}_{k_{S_0T_0-Rel}} \quad Eq. 4$$

255 where  $k_{S_0T_0}$  is the apparent permeability for a given saturation degree  $S_w$ .  $q$  and  $m$  are the van  
 256 Genuchten parameters, which depend on material characteristics.

257 For the concrete tested in this study, the apparent permeability  $k_0$  obtained from the van  
 258 Genuchten model on samples conditioned at less than 60 °C was equal to  $13 \cdot 10^{-17} \text{ m}^2$ .  $q$  and  $m$   
 259 were respectively equal to 3.7 and 0.5. These values are in good agreement with usual literature  
 260 values ( $q$  lies between 3.5 and 5 and  $m$  is equal to 0.5 [35, 65-67]). Apparent permeability in  
 261 the dry state (0% of saturation) after drying at 105 °C was also measured at the end of the  
 262 experimentation. It was equal to more than  $18.5 \cdot 10^{-17} \text{ m}^2$  (with a standard deviation of about  
 263  $6 \cdot 10^{-17} \text{ m}^2$ ). The difference between the permeability deduced from the van Genuchten model  
 264 and the permeability measurement after the conditioning at 105 °C can be explained by the  
 265 impact of the damage on transfer properties of concrete when the temperature of conditioning  
 266 becomes too high. For such temperatures, the origin of the damage changes: considerable  
 267 thermo-chemical damage is then combined with hydric damage. This leads to strong  
 268 nonlinearity for damage (Figure 1) and for permeability.

269

### 270 3.2.2 Evolution of permeability just after thermal loading

271 Permeability measured on samples just after the thermal loading (K1) is presented in Figure 4  
272 for the four saturation degrees.

273 The aim of this part was to quantify the permeability variation measured on dry samples. It was  
274 only achieved for 150 and 200 °C (specimens exposed to 80 °C were not dry at the end of the  
275 temperature exposure and are thus not analysed in this part). A thermal loading of 200 °C led  
276 to a greater increase in permeability than 150 °C (Figure 4). Such results can be explained by  
277 the increase in the thermo-chemical damage between 150 and 200 °C.

278

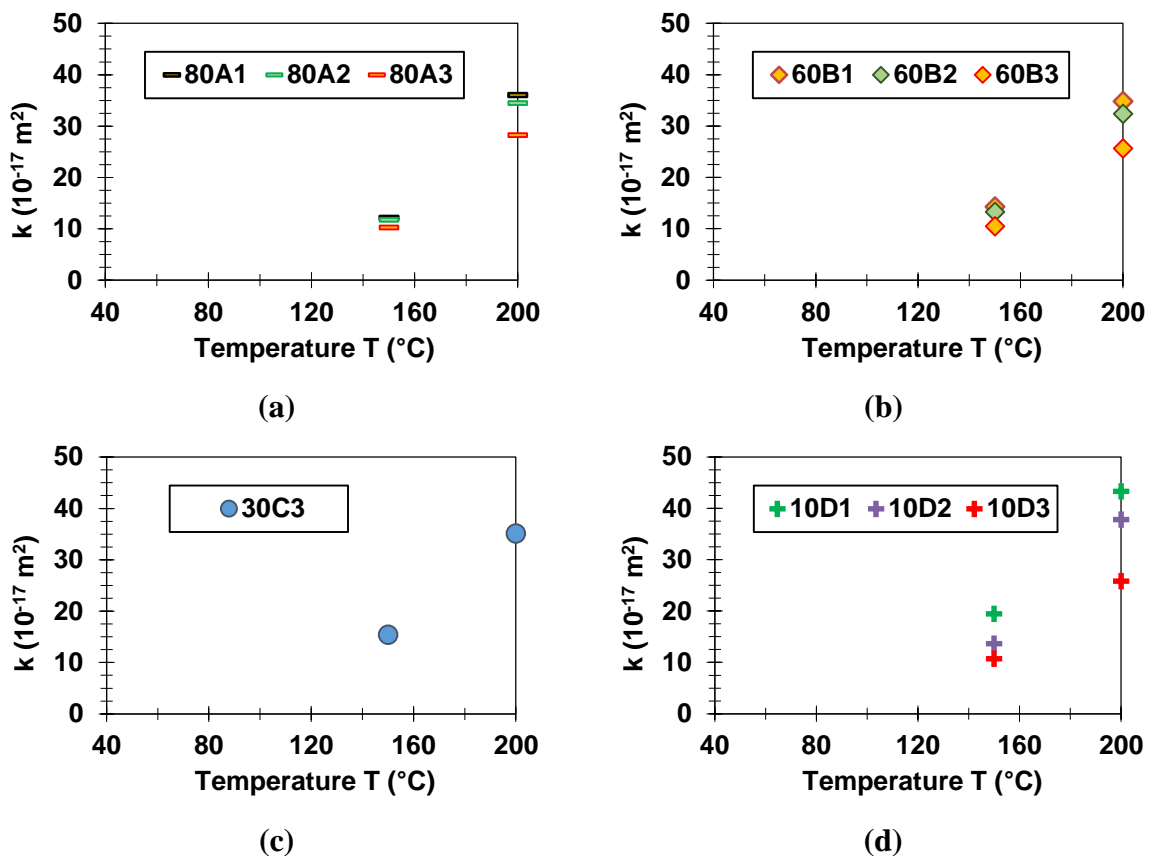


Figure 4. Apparent permeability just after thermal loading at 150 and 200 °C for four initial saturation degrees

279 After thermal loading at 150 and 200 °C, the permeability of samples lies in the same range  
280 whatever their initial saturation degree (Figure 4). As for mechanical characterization, samples  
281 lost free and combined water quickly and the difference of initial saturation degree had little  
282 impact. The temperature of loading seems to play the major role in the permeability increase  
283 when permeability is measured in the dry state. To distinguish the impact of the saturation

284 degree of concrete during measurement and the effect of damage, permeability measurements  
285 were performed after resaturation (protocol K2). This is presented in the following section.

### 286 3.2.3 *Evolution of permeability after resaturation*

287 The permeability of the samples measured after the resaturation of the concrete with the same  
288 quantity of water (protocol K2) is presented in Figure 5.

289 Apparent permeability is small, and lower than permeability obtained for K1 in Figure 4. This  
290 result was to be expected as the saturation degree increased between the two protocols of  
291 measurement. Large relative increases have to be noted for high saturation degrees (Figure 5).  
292 For saturation degrees of concrete equal to 60 or 80% during measurement (samples 60Bi and  
293 80Ai in Figure 5), permeability was hardly measurable at initial temperature because very little  
294 flow could cross the samples. However, after exposure to 150 and 200 °C, flow was clearly  
295 detectable while the saturation degree was still high (Figure 5).

296 Thermal loading below 100 °C seems to have little impact on air permeability. As samples were  
297 conditioned at 50°C to reach their target saturation degree the impact of thermal stress on  
298 percolation paths between 50°C and the thermal loading at 80°C was not sufficient to lead to a  
299 change in permeability. After thermal loading at 150 °C and 200 °C, the permeability increased  
300 for all the saturation degree as already observed for dry concrete in [68]. Physicochemical  
301 degradation and mechanical damage increased the accessible porosity and modified the  
302 concrete microstructure, so an increase of permeability was observed.

303

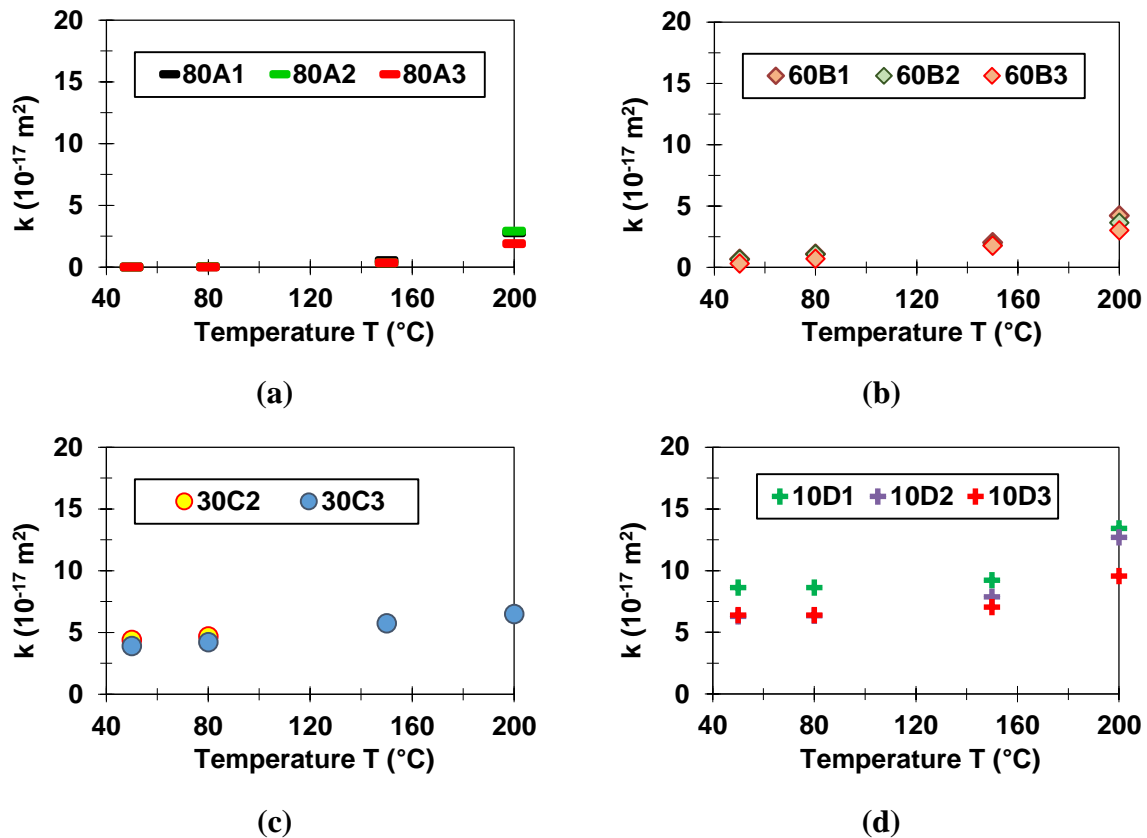


Figure 5. Apparent permeability as a function of the temperature for four initial saturation degrees

305 The flow  $Q(T)$  measured during permeability tests after thermal loading can be compared to  
 306 the flow  $Q(50)$ , which is the flow measured for partially saturated samples before the thermal  
 307 loading. Results are presented in Figure 6. For low saturation degrees, the proportion of air flow  
 308 in the initial percolation path of the concrete is higher than 60%, while, at high saturation  
 309 degrees, the air flow occurs mainly in new paths induced by the thermal loading (Figure 6).  
 310 This information is important for the evaluation of leakage from damaged structures in real  
 311 environmental conditions.

312 Figure 6 is also interesting for the quantification of the cracking induced by the temperature.  
 313 Crack openings were sufficient to allow significant transfer despite the high water content.  
 314 Because of their size and their connection, these paths were drained even at high water contents.  
 315 The air permeability is known to be a sensitive technique to detect damage [69]. For high  
 316 saturation degrees, this experimentation shows that very small defects, which may have  
 317 negligible impact on the mechanical properties, lead to large impact on the permeability. It  
 318 confirms thus the high sensitivity of this measure to cracking, especially in saturated concrete.

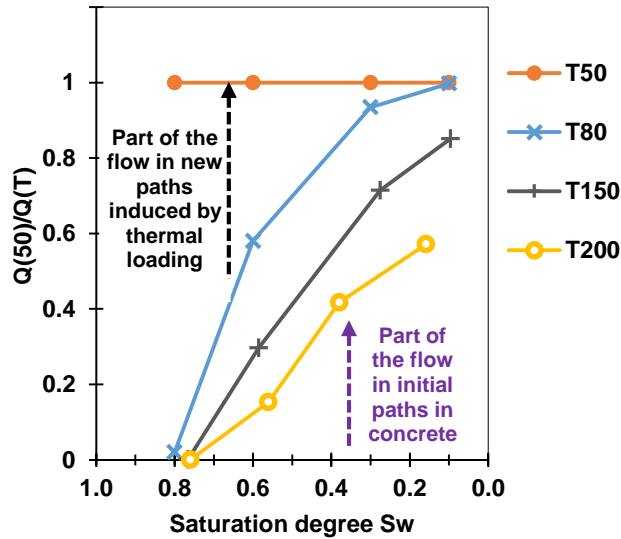


Figure 6. Ratio of the flow in samples before and after thermal loading versus the saturation degree during permeability measurement

319

## 320 4 Analysis

### 321 4.1 Relative change in modulus

322 The relative change in modulus is usually used to evaluate the concrete damage due to  
 323 mechanical loading. Thermal loading leads also to relative change in modulus but the  
 324 modifications are not only caused by mechanical reasons. The evolution of the modulus in  
 325 concrete submitted to elevated temperatures is due to the combination of many mechanisms  
 326 (cracking, physicochemical modifications, porosity saturation by pore solution). The use of  
 327 relative change in modulus to evaluate the damage induced by elevated temperature in concrete  
 328 is thus questionable. However, the part really due to damage in the modulus evolution is  
 329 difficult to separate to the other contributions by usual measurable parameters. Therefore, the  
 330 damage due to thermal loading is evaluated from relative change in modulus as is usual in  
 331 modelling approaches presented in literature [10, 22]. It has not to be interpreted as the usual  
 332 mechanical damage but as a global evaluation of the relative change in modulus due to all the  
 333 mechanisms involved in temperature exposure. In the future, mesoscopic modelling could be  
 334 used to have a better evaluation of the effects of each mechanism on the evolution of the  
 335 modulus, and to distinguish clearly the mechanical damage to the contribution of other  
 336 mechanisms, as particularly the water saturation of concrete porosity.

337 4.1.1 Impact of drying

338 The evolution of the modulus with the saturation degree was evaluated through  $\delta_H$  regardless  
 339 of the nature of its origins (physicochemical and/or mechanical):

$$\delta_H = 1 - \frac{E_S}{E_{100\%}} \quad \text{Eq. 5}$$

340 where  $\delta_H$  is used to quantify the modulus evolution due to drying [70],  $E_S$  is the modulus at a  
 341 given saturation degree (after drying),  $E_{100\%}$  is the initial modulus after 60 days in lime water  
 342 and before drying, taken as a reference.

343 For saturation degrees higher than 30%, the damage increased linearly with the saturation  
 344 degree. The decrease of modulus was slightly greater than 6% for a degree of saturation of  
 345 about 30% (Figure 7). This decrease is small. The impact of the water loss on the Young  
 346 modulus during exposure of the concrete to the chosen temperature appears to be small until  
 347 30% of saturation is reached (drying at 60 °C).

348 The linearity of the damage induced by drying can be evaluated as a function of the saturation  
 349 degree as follows:

$$\delta_H = H \cdot (1 - S_w) \quad \text{Eq. 6}$$

350 The coefficient H thus defined is the rate of loss of rigidity of the material due to hydric damage.  
 351 It can be used to evaluate the sensitivity of the concrete rigidity to drying: when H is high, the  
 352 concrete modulus is more sensitive to loss of water.

353 The parameter H was calibrated using the experimental measurements. It was equal to 0.10 for  
 354 the concrete tested in this work, which is in good accordance with literature results (Table 2).

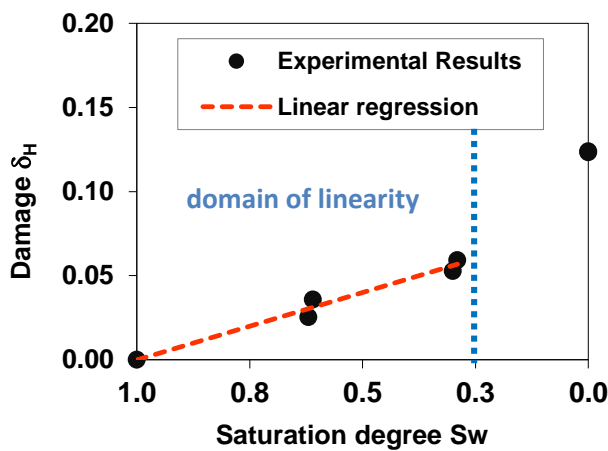


Figure 7. Damage  $\delta_H$  versus saturation degree

355



**Table 2.** Value of H deduced from literature data

E/C	Concrete samples		Deduced value of H	Authors
	Rc100% (MPa)	E100% (GPa)		
0.57	45	41	0.11	Bucher et al. [71]
0.64	32	25	0.05	Vu [72]

357 Most of experimental works on the evolution of Young modulus with saturation degree exhibit  
 358 linearity between 100% and 20% of saturation [52, 57, 58]. For very dry materials (below 20%),  
 359 the correlation between modulus and saturation can be linear [52, 58] or nonlinear [58]  
 360 according to the concrete composition and test conditions. Particularly, the effect of the  
 361 aggregate size on the opening of cracks due to cement paste restraint by aggregate [3] can  
 362 explain a brutal increase in the impact of saturation on modulus for concrete containing coarse  
 363 aggregate.

364 In the present work, the evolution of damage with the degree of saturation is no longer linear  
 365 below 30%. In the dry state (obtained at 105 °C), the damage increases rapidly for a small  
 366 difference of saturation. The loss of linearity of the Young modulus evolution indicates the  
 367 creation of a cracking network having a marked impact on the permeability. For 0% of  
 368 saturation (drying temperature equal to 105 °C), the concrete damage is mainly due to thermo-  
 369 chemical mechanisms. Drying at high temperatures increases the importance of microcracking  
 370 (density, width, length...) [43]. The density of cracking increases significantly between 50 °C  
 371 and 105 °C [43]. It can explain the non-linearity of damage obtained for very small saturation  
 372 degrees. However, the correlation between modulus and saturation cannot be determined for  
 373 low saturation degrees as the number of measurements is not sufficient. Future works on the  
 374 mechanical behaviours of concrete submitted to severe drying should focus on this domain of  
 375 saturation.

376 Above 30% of saturation, the damage is supposed to be mainly due to water departure (impact  
 377 of drying for temperatures lower than 60 °C). To quantify the damage principally associated  
 378 with the water departure, it seems appropriate to keep the linear relation of the Young modulus  
 379 with saturation degree. Although the nature of the cracking is different, damage of about 5%  
 380 (equal to the drying damage at 30% of saturation) caused by a compressive load usually has  
 381 little impact on the permeability, while damage of about 12% (equal to the drying damage at  
 382 0% of saturation) can increase the permeability by a factor lying between 2 and 5 [68, 70].

383 The hydric damage, as defined in this paper, does not integrate the impact of cycles of drying  
 384 and re-humidification that can occur in the material on site. Additional studies are necessary to  
 385 analyse the impact of the life cycle of concrete on this property.

386

#### 387 4.1.2 Impact of elevated temperatures

388 The evolution of the modulus with the temperature of the thermal loading according to the  
 389 initial saturation degree was evaluated through  $\delta_{T,H_0}$  regardless of the nature of its origins:

$$\delta_{T,H_0} = 1 - \frac{E_{T,S}}{E_{S_0}} \quad \text{Eq. 7}$$

390 where  $\delta_{T,H_0}$  is used to quantify the modulus evolution due to thermal loading in comparison  
 391 with the state of samples just before the thermal loading at saturation degree  $S_w = S_0$ .  $E_{S_0}$  and  
 392  $E_{T,S}$  are the modulus of concrete before and after the thermal loading, respectively.

393 Literature data indicate that a linear evolution can be established for the evolution of the  
 394 decrease of modulus according to temperature [73]. Figure 8 illustrates the results obtained in  
 395 this study. They are in good agreement with the results presented in [22].

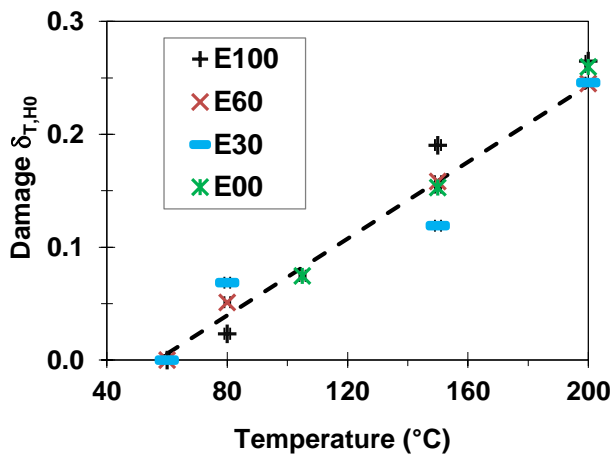


Figure 8. Evolution of the thermo-chemical damage as a function of exposure temperature

396 The linear regression deduced from the experiments (Figure 8) is:

$$\delta_{T,H_0} = A_{TH} \cdot T + B_{TH} \quad \text{Eq. 8}$$

397 where  $A_{TH}$  and  $B_{TH}$  are calibration parameters. In this study,  $A_{TH}$  was equal to 0.0017 and  $B_{TH}$   
 398 to -0.0965. These values are close to parameters obtained in Schneider's work [74]. In this  
 399 study, dried concrete was subjected to temperatures increasing from 20 to 800 °C [74]. From  
 400 his data,  $A_{TH}$  and  $B_{TH}$  can be evaluated at 0.0011 and -0.0376 respectively.

401 In the last part of the paper, these results are used to analyse the correlation between the thermo-  
402 chemical damage and the evolution of the permeability induced by the exposure to temperature.

403

## 404 **4.2 Permeability**

### 405 *4.2.1 Relative permeability after thermal loading*

406 The evolution of the permeability highlighted in the previous part was caused by the  
407 combination of two mechanisms: the impact of the saturation degree on initial transfer paths  
408 and the impact of the thermo-chemical damage on the increase of the transfer path (due to  
409 decomposition of hydrates and/or cracking). In order to distinguish the two phenomena, the  
410 relative permeability  $k_{TH,Rel}$  is defined in this part. In the experiments, it was almost impossible  
411 to obtain exactly the same saturation degree before and after the thermal loading and  
412 resaturation. For partially saturated concrete, a small difference of saturation degree can lead to  
413 a large variation of permeability (Figure 3). As the saturation degree was not exactly the same,  
414 experimental permeability values could not be directly compared to define  $k_{TH,Rel}$ . To  
415 circumvent this difficulty in the analysis, the permeability was normalized taking into account  
416 the saturation degree of concrete:  $k_{TH,Rel}$  was related to the reference state obtained from the  
417 van Genuchten model and has been presented in Figure 3-b. Thus, the impact of the saturation  
418 degree was evaluated from the van Genuchten model and the impact of the thermo-chemical  
419 damage could be highlighted. For a given saturation degree  $S_0$ :

$$k_{TH,Rel} = \frac{k_{S_0T}}{k_{S_0T_0}} \quad Eq. 9$$

420 where  $k_{S_0T}$  is the permeability for a given saturation state after exposure to the chosen  
421 temperature T (80, 150 and 200 °C) and  $k_{S_0T_0}$  is the reference permeability, considering the  
422 effect of the saturation degree by Eq. 4. Thus,  $k_{TH,Rel}$  does not depend on the saturation degree  
423 of the sample during the permeability measurement. If the permeability is not modified by the  
424 thermal loading,  $k_{TH,Rel}$  is equal to 1. If this relative permeability is higher than 1, the difference  
425 has been induced by the temperature.

426 Figure 9 presents the relative permeability  $k_{TH,Rel}$  for samples just after the thermal loading  
427 (protocol K1).

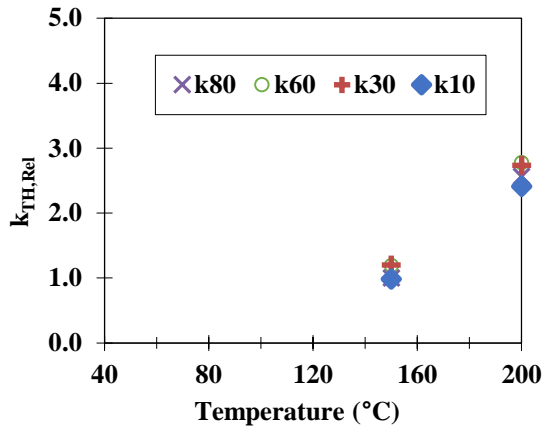


Figure 9. Relative permeability just after the thermal loading (K1)

428 For measurements performed just after the thermal loading (Figure 9):

429 - The exposure at 150 °C had a negligible impact on permeability:  $k_{TH,Rel}$  is about 1.

430 - For the loading at 200 °C,  $k_{TH,Rel}$  lies between 2 and 3. The temperature loading induced  
 431 thermo-chemical damage in the concrete but the consequences in terms of permeability  
 432 remain moderate at this temperature level.

433 For the two temperatures, the large effect on permeability shown in Figure 4 was mainly due to  
 434 the decrease of the water content of the concrete.

435 In contrast, the impact of thermal loading on the permeability of partially saturated concrete  
 436 was significant (Figure 10).

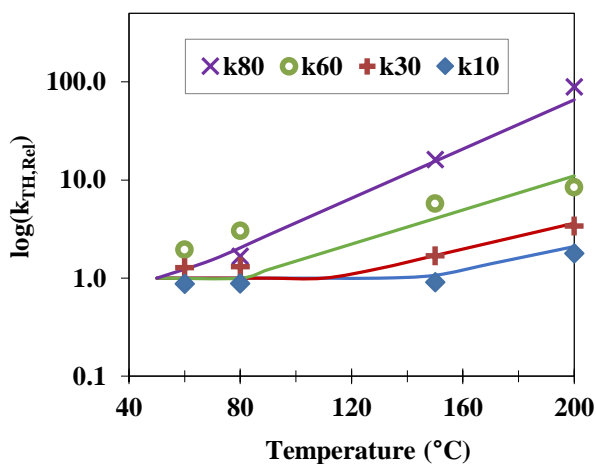


Figure 10. Relative permeability after resaturation (K2): experimentation and empirical laws

437 For the lowest temperature, all the relative permeability  $k_{TH,Rel}$  must be equal to 1 as the  
 438 samples have not been subjected to the thermal loading. However, the samples with an initial  
 439 saturation degree of 60% show a mean relative permeability of about 2. This is due to an

440 approximate evaluation of  $k_{S_0T_0}$  by the van Genuchten model (differences between the model  
441 and experimental results in Figure 3-b). For the same reason, at Sw equal to 30%,  $k_{TH,Rel}$  is  
442 slightly higher than 1 because the van Genuchten estimation of experimental permeability is  
443 too low. At Sw = 10%,  $k_{TH,Rel}$  is less than 1 because of overestimation by the van Genuchten  
444 model.

445 For measurements at high saturation degrees of (60 and 80%), the impact of thermal loading at  
446 80 °C on the permeability is quite small. If it exists, it is of the same order as the discrepancy  
447 due to the use of the van Genuchten model as explained just above. However, exposure to 200  
448 °C leads to a significant increase in permeability. The impact of the thermal loading on  
449 permeability decreases when the initial saturation degree is lower. For high water content,  
450 significant thermo-chemical damage occurs. Even if the concrete is resaturated with the same  
451 water content, the water is not able to fill all the new paths created during the exposure to  
452 temperature. These new paths are probably micrometric and interconnected and can be drained  
453 even at high relative humidity. The consequence is a significant increase in permeability for  
454 concrete with a high saturation degree. This result is important for the evaluation of the leakage  
455 of damaged structures after exposure to elevated temperatures. Such experimental data are  
456 necessary to evaluate the capacity of mesoscopic modelling considering the impact of thermal  
457 damage on permeability [18] for partially saturated concrete.

#### 458 4.2.2 *Combination of saturation and thermal damage impacts*

459 Phenomenological relationships have been proposed to evaluate the permeability of damaged  
460 concrete in relation to the initial permeability and to the temperature [7, 75]:

$$k = k_0 \exp[C_T(T - T_0)] \quad \text{Eq. 10}$$

461 where  $k_0$  is the initial permeability of concrete subjected to the reference temperature  $T_0$  and  $C_T$   
462 is a parameter that can be calibrated using experimental results.

463 The analysis proposes here to combine the van Genuchten model (Eq. 4) with the law presented  
464 in Eq. 10 to separate the impact of the saturation degree at the time of permeability measurement  
465 from the effect of the thermal damage.

466 With this objective, two parameters are defined:

- 467 -  $T_S$ : the temperature limit above which the thermal loading leads to an increase in  
468 permeability.

469 -  $C_{T,S}$  is the coefficient  $C_T$  in Eq. 10 but with dependence on the initial saturation degree at  
 470 the beginning of the thermal loading.

471 The following equation is thus proposed to evaluate the apparent permeability:

$$k_{S_0T} = \underbrace{k_0(1 - Sw)^q(1 - Sw^{1/m})^{2m}}_{k_{S_0T_0}} \cdot \underbrace{\exp[C_{T,S}\langle T - T_S \rangle]}_{k_{TH,Rel}} \quad Eq. 11$$

472 where  $k_{S_0T_0}$  is given by the van Genuchten model,  $\langle T - T_S \rangle = 0$  when  $T_S > T$  and  $\langle T - T_S \rangle =$   
 473  $T - T_S$  when  $T_S < T$ .

474  $C_{T,S}$  and  $T_S$  are both calibrated to reproduce the results for each saturation degree (Figure 10)  
 475 and to give a gradual trend of their evolution with the saturation degree according to:

$$C_{T,S} = A_C \exp(B_C \cdot Sw) \quad Eq. 12$$

$$T_S = A_T \exp(B_T \cdot Sw) \quad Eq. 13$$

476 where  $A_C$ ,  $B_C$ ,  $A_T$ ,  $B_T$  are calibration parameters. For the concrete tested in this study,  $A_C$ ,  $B_C$ ,  $A_T$   
 477 and  $B_T$  are equal to 0.012, 0.89, 163, and -1.12 respectively.

478 The literature reports values of  $C_T$  lying between 0.01185 and 0.02019 [7] (for tests performed  
 479 on dried samples,  $S_0 = 0\%$ ). With Eq. 12,  $C_{T,S}$  is equal to 0.012 for  $S_0 = 0\%$ . It is thus in good  
 480 agreement with the literature values.

481 To obtain a good calibration (Figure 10), it seems important to replace the reference temperature  
 482  $T_0$  in Eq. 10 by a limit temperature  $T_S(Sw)$  (Eq. 13). This limit temperature depends on the  
 483 initial saturation degree. Below this temperature, the thermal loading has no significant impact  
 484 on the permeability. This modification was necessary to obtain a good representation of all the  
 485 measurements.

486 For the permeability measured with the protocol K1 (measurements on dried samples just after  
 487 the thermal loading), the proposed model (Eq. 11) leads to  $k_{TH,Rel}$  equal to 1 and 1.8 for  
 488 temperatures of 150 °C and 200 °C, respectively. Figure 9 indicates that, for  $T = 150$  °C,  $k_{TH,Rel}$   
 489 lies around 1 and, for  $T = 200$  °C,  $k_{TH,Rel}$  is about 2.5. The proposed relationship leads to a  
 490 suitable evaluation of the experimental results of the first protocol.

491 In order to assess the rate flow of their structures, engineers in charge of the management of  
 492 containment structures need phenomenological laws to evaluate the concrete permeability  
 493 submitted to various loading. Such laws can also be useful for macroscopic modelling of these  
 494 very large structures for which precise evaluation of cracks can be complex or too time  
 495 consuming. As shown by the present analysis, the combination of two laws of the literature give  
 496 a correct evaluation of this transfer property after thermal loading according to its saturation

497 degree before exposure. The relationships proposed for the dependence of the parameters of  
 498 these laws on the saturation degree allows their generalization to various environmental  
 499 conditions. In this approach, concrete is supposed homogeneous without distinction of the  
 500 different phases of the material and of the cracks induced by the thermal loading. More precise  
 501 modelling could be helpful to better evaluate the part of the flow in the concrete porosity and  
 502 in new paths formed by cracking resulting of the thermal loading. Such modelling can also be  
 503 very interesting to evaluate the impact of the mechanical properties of concrete exposed to such  
 504 loading on the increase of transfer property. In the future, modelling combining mechanical and  
 505 transfer considerations [76] should be used to propose a more complete and precise evaluation  
 506 of the effects of thermal loading on the transfer properties of concrete.

### 507 4.3 Discussion

#### 508 4.3.1 Correlation between relative permeability and relative change in modulus

509 As the thermo-chemical damage has a linear relation with the temperature (Figure 8), the  
 510 correlation between permeability and damage can be drawn from Eq. 8 and Eq. 11:

$$k_{S_0,T} = \underbrace{k_0(1-Sw)^q(1-Sw^{1/m})^{2m}}_{k_{S_0T_0}} \cdot \underbrace{\exp\left[C_{T,S}\left(\frac{\delta_{T,H_0} - B_{TH}}{A_{TH} - T_S}\right)\right]}_{k_{TH,Rel}} \quad \text{Eq. 14}$$

511 where  $k_{S_0T_0}$  is given by the van Genuchten model.

512  $A_{TH}$ ,  $B_{TH}$ ,  $C_{T,S}$  and  $T_S$  have been calibrated in the previous parts (Eq. 8, Eq. 12 and Eq. 13).

513 The relative permeability  $k_{TH,Rel}$  as expressed in Eq. 14 is plotted in Figure 11 for comparison  
 514 with the experimental data obtained in this program.

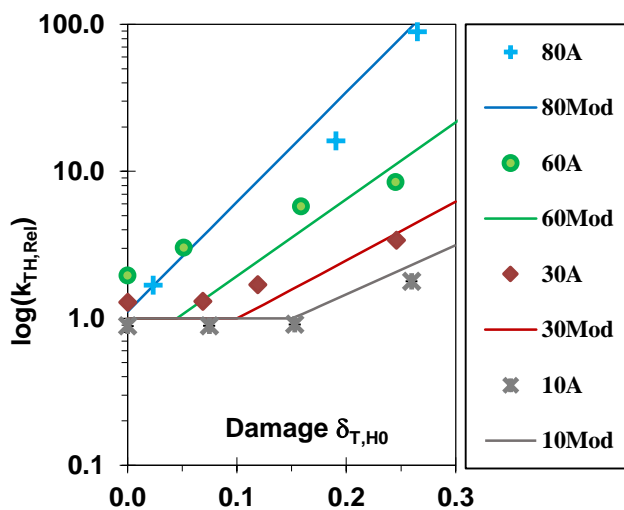


Figure 11. Comparison between experimental results and proposed model

515 The correlations between the relative permeability and the damage induced by the thermal  
516 loading can thus be deduced from the previous relationships (Figure 11). For low saturation  
517 degrees, the exposure to temperature leads to considerable damage but to low permeability  
518 variations. For small saturation degrees, the water in the percolation path is released and the  
519 initial permeability is already high. The relative increase after the temperature exposure is thus  
520 not so marked as for high saturation degrees.

521 Empirical relations (Eq. 14) can be used to evaluate the relative permeability with quite good  
522 accuracy, in relation to usual experimental dispersion for permeability and damage assessments.  
523 The distinctions between the experimental results and the predictions for the smallest damage  
524 are due to the evaluation of  $k_{TH,Rel}$  as explained in the previous part (particularly for concrete  
525 at 60% of saturation).

526 Because of the dependence of the correlation on the saturation degree, the relative permeability  
527 cannot be directly deduced from the damage. For example, for 25% damage, the relative  
528 permeability lies between 2 and 100 according to the saturation state. For measurements on site,  
529 this correlation can be used to evaluate the relative permeability from indirect measurements.  
530 If the damage and the saturation degree of in situ concrete are known, such experimental  
531 relationships could allow the relative permeability to be evaluated without direct measurement  
532 of the permeability. Additional work will be necessary to confirm this method.

#### 533 4.3.2 Comparison with literature

534 One of the objectives of this study was to analyse the correlation between relative permeability  
535 and damage induced by thermal loading. In the literature, such results are scarce for thermal  
536 loading lower than 200 °C and damage lower than 0.2, but several studies have analysed the  
537 impact of mechanical loading on permeability in this range of damage [31, 77]. As the damage  
538 due to mechanical and thermal loading has different origins, the consequences in terms of  
539 induced cracking and thus permeability variation have to be compared.

540 Figure 12 compares the results of the present study obtained on concrete subjected to thermal  
541 loading and the results of concrete subjected to mechanical compressive loading [31, 77]  
542 (obtained on concrete dried at 105 °C until constant mass). In [31, 77], the damage is calculated  
543 from  $(E_0 - E_d)/E_0$  with  $E_0$ , the modulus before the mechanical loading and  $E_d$ , the modulus after  
544 the mechanical loading. The relative permeability  $k_{Rel}$  is the ratio between the apparent  
545 permeabilities measured after and before the loading. For the present study, only the four trends  
546 obtained with the previous equation have been kept, to simplify the figure.



547 The nature and location of the damage is different according to the nature of the loading.  
 548 However, thermal and mechanical loadings seem to induce similar correlations between relative  
 549 permeability after loading and damage evaluated from the Young modulus (Figure 12).  
 550 The evolution of permeability according to damage is of the same order whatever the origin of  
 551 the damage (mechanical or thermal). For dry concrete, mechanical loading seems to cause  
 552 higher relative permeability than thermal loading.  
 553 As for compressive loading [31, 77-79], thermal loading shows a threshold of damage for  
 554 unsaturated concrete. Below this threshold, the damage induced by thermal loading does not  
 555 impact the permeability. The new paths induced by the thermal loading are not coalescent or  
 556 not sufficiently wide to impact the permeability until this damage threshold is reached. It can  
 557 be related to the threshold of crack width observed for the effect of mechanical loading on  
 558 permeability [78].  
 559 For most of the experimental works, only small increases of permeability were noted for  
 560 damage lower than 0.06. This is the value of damage obtained for drying to 30% of saturation  
 561 (Figure 7). Drying from 60% to 30% could lead to a small increase in permeability (the  
 562 maximum relative permeability is 1.8 for damage of 0.06 for all the experimental studies  
 563 presented in Figure 12).  
 564

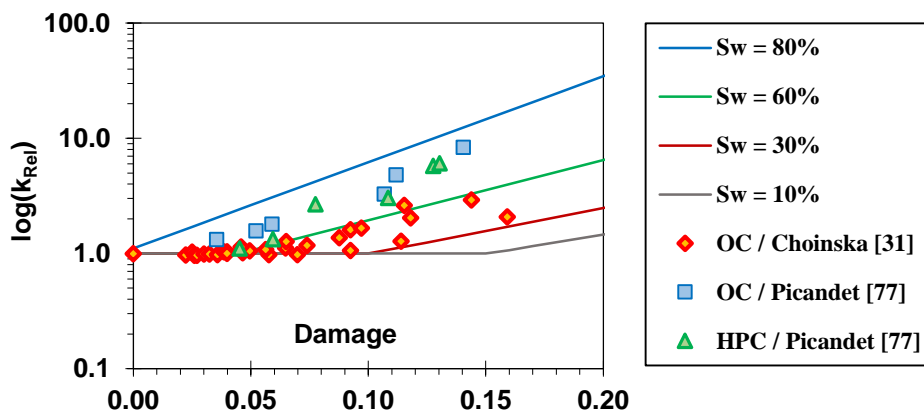


Figure 12. Evolution of permeability with damage after thermal loading (lines) and after mechanical loading (points, OC = ordinary concrete, HPC = High Performance Concrete) from [31, 77]

565

## 566 **5 Conclusion**

567 The findings presented in the paper can contribute to the knowledge of the evolution of concrete  
568 permeability after exposition to elevated temperatures. It deals also with the correlation between  
569 concrete damage and permeability after such loading.

570 Permeability of partially saturated concrete through air permeability measurement has been  
571 analysed. If the permeability is measured just after the thermal loading and drying, the initial  
572 saturation state of the concrete seems to have little impact. The permeability is then mainly  
573 impacted by the saturation state during measurement. It is thus necessary to separate the effect  
574 of thermal damage from the effect of saturation. It can be obtained after resaturation of concrete  
575 to the initial saturation degree. Permeability measurement after resaturation shows small  
576 modifications for concrete with a low saturation degree and large modifications for saturated  
577 concrete. During the thermal loading, the temperature has to be high enough to induce  
578 significant damage. This temperature limit, under which the thermal loading has no impact on  
579 concrete permeability, is dependent on the saturation degree. When the saturation degree is  
580 high, even low thermal loading may induce an increase of permeability while, when the  
581 saturation degree is low (lower than 30%), the thermal loading has to be more severe (above  
582 100°C) before leading to a significant increase of permeability.

583 After exposition to elevated temperatures, air flow occurs mainly in the initial percolation path  
584 of concrete for low initial saturation degrees but the air flow occurs in new paths induced by  
585 the exposure to temperature for high initial saturation degrees. The degree of saturation of  
586 concrete on site is usually high, concrete saturated at 80% can be permeable to air after thermal  
587 loading, which was not the case before exposure. For concrete with high saturation degree, even  
588 a small damage can lead to large permeability increase.

589 To obtain a good representation of all the saturation degrees (from 10% to 100%), it has been  
590 necessary to revisit the usual empirical relations between permeability and temperature. A van  
591 Genuchten model cannot be used alone to predict the permeability of saturated concrete  
592 damaged by thermal loading. It can be combined with a phenomenological model to account of  
593 the increase of permeability due to thermo-chemical damage. Adaptations of existing laws have  
594 been proposed in this paper to take the impact of the initial saturation degree into account.

595 These experimental data and analysis are necessary to obtain relevant modelling to predict the  
596 behaviour of structures in field after thermal loading due, for example, to accidental situation.

597

## 598 **6 Acknowledgements**

599 The authors acknowledge the financial support provided by the project “Non-destructive  
600 evaluation of containment of nuclear power plants” (ENDE) financed by the Programme  
601 Investissement d’Avenir (PIA – Centre National de la Recherche Scientifique, délégation  
602 Provence et Corse, France). The opinions presented in this paper reflect only those of the  
603 authors and do not necessarily represent the opinions of the funding agencies.  
604

## 605 **7 References**

- 606 [1] Z. P. Bazant and P. C. Prat, “Effect of Temperature and Humidity on Fracture Energy  
607 of Concrete,” *Mater. J.*, vol. 85, no. 4, pp. 262–271, 1988.
- 608 [2] N. Burlion, I. Yurtdas, and F. Skoczylas, “Comportement mécanique et séchage de  
609 matériaux à matrice cimentaire ; Comparaison mortier - béton,” *Rev. Fr. Génie Civ.*, vol. 7, no.  
610 2, pp. 145–165, 2003.
- 611 [3] M. Szczesniak, T. Rougelot, N. Burlion, J. Shao, “Compressive strength of cement-  
612 based composites : Roles of aggregate diameter and water saturation degree,” *Cem. Concr.*  
613 *Compos.*, Vol. 37, pp. 249–258, 2013.
- 614 [4] I. Yurtdas, N. Burlion, and F. Skoczylas, “Experimental characterisation of the drying  
615 effect on uniaxial mechanical behaviour of mortar,” *Mater. Struct.*, vol. 37, no. 3, pp. 170–176,  
616 2004.
- 617 [5] S. Divya Rani, M. Santhanam, “Influence of moderately elevated temperatures on  
618 engineering properties of concrete used for nuclear reactor vaults”, *Cem. Concr. Compos.*, vol.  
619 34, pp. 917–923, 2012.
- 620 [6] Y. Pei, F. Agostini, and F. Skoczylas, “The effects of high temperature heating on the  
621 gas permeability and porosity of a cementitious material,” *Cem. Concr. Res.*, vol. 95, pp. 141–  
622 151, 2017.
- 623 [7] D. Gawin, C. Alonso, C. Andrade, C. E. Majorana, and F. Pesavento, “Effect of damage  
624 on permeability and hygro-thermal behaviour of HPCs at elevated temperatures: Part 1.  
625 Experimental results,” *Comput. Concr.*, vol. 2, no. 3, pp. 189–202, 2005.
- 626 [8] N. Hearn, “Effect of Shrinkage and Load-Induced Cracking on Water Permeability of  
627 Concrete,” *Mater. J.*, vol. 96, no. 2, pp. 234–241, 1999.
- 628 [9] N. Burlion, F. Skoczylas, and T. Dubois, “Induced anisotropic permeability due to  
629 drying of concrete,” *Cem. Concr. Res.*, vol. 33, no. 5, pp. 679–687, 2003.
- 630 [10] S. D. Pont, B. A. Schrefler, and A. Ehrlacher, “Intrinsic Permeability Evolution in High  
631 Temperature Concrete : An Experimental and Numerical Analysis,” *Transp. Porous Media*, vol.  
632 60, no. 1, pp. 43–74, 2004.
- 633 [11] M. Lion, F. Skoczylas, Z. Lafhaj, and M. Sersar, “Experimental study on a mortar.  
634 Temperature effects on porosity and permeability. Residual properties or direct measurements  
635 under temperature,” *Cem. Concr. Res.*, vol. 35, no. 10, pp. 1937–1942, 2005.

- 636 [12] T. Suzuki, K. Takiguchi, and H. Hotta, "Leakage of gas through concrete cracks," Nucl.  
637 Eng. Des., vol. 133, no. 1, pp. 121–130, 1992.
- 638 [13] G. A. Khoury, B. N. Grainger, and P. J. Sullivan, "Transient thermal strain of concrete:  
639 literature review, conditions within specimen and behaviour of individual constituents," Mag.  
640 Concr. Res., vol. 37, no. 132, pp. 131–144, 1985.
- 641 [14] I. Hager, "Behaviour of cement concrete at high temperature," Bull. Pol. Acad. Sci.  
642 Tech. Sci., vol. 61, no. 1, pp. 145–154, 2013.
- 643 [15] A. Noumowé, "Effet de hautes températures (20-600°C) sur le béton : cas particulier du  
644 béton à hautes performances," Ph.D. Thesis, INSA de Lyon, 1995.
- 645 [16] T. Z. Harmathy, "Thermal properties of concrete at elevated temperatures", J. Mater.,  
646 1970.
- 647 [17] P. Klieger, J. F. Lamond, "Significance of test and properties of concrete and concrete-  
648 making materials", ASTM Publication, USA, 1994.
- 649 [18] F. Grondin, H. Dumontet, A. Ben Hamida, H. Boussa, "Micromechanical contributions  
650 of the behaviour of cement-based materials: Two-scale modelling of cement paste and concrete  
651 in tension at high temperatures", Cem. Concr. Compos., vol. 33, pp. 424–435, 2011.
- 652 [19] M. V. G. de Morais, A. Noumowé, M. Kanema, J.-L. Gallias, and R. Cabrillac,  
653 "Transferts thermo-hydriques dans un élément en béton exposé à une température élevée:  
654 Approches numérique et expérimentale," 24ème Rencontres Univ. Génie Civ. AUGC06, pp.  
655 1–10, 2006.
- 656 [20] J.-C. Mindeguia, P. Pimienta, A. Noumowé, and M. Kanema, "Temperature, pore  
657 pressure and mass variation of concrete subjected to high temperature — Experimental and  
658 numerical discussion on spalling risk," Cem. Concr. Res., vol. 40, no. 3, pp. 477–487, 2010.
- 659 [21] Z. P. Bazant, "Constitutive equation for concrete creep and shrinkage based on  
660 thermodynamics of multiphase systems," Matér. Constr., vol. 3, no. 1, pp. 3–36, 1970.
- 661 [22] D. Gawin, F. Pesavento, and B. A. Schrefler, "Modelling of hygro-thermal behaviour  
662 of concrete at high temperature with thermo-chemical and mechanical material degradation,"  
663 Comput. Methods Appl. Mech. Eng., vol. 192, no. 13–14, pp. 1731–1771, 2003.
- 664 [23] Z. P. Bazant and F. H. Wittmann, "Creep and shrinkage in concrete structures," 1982.
- 665 [24] D. Gardner, "Experimental and numerical studies of the permeability of concrete,"  
666 Ph.D. Thesis, Cardiff University, 2005.
- 667 [25] M. A. Sanjuán and R. Muñoz-Martialay, "Oven-drying as a preconditioning method for  
668 air permeability test on concrete," Mater. Lett., vol. 27, no. 4–5, pp. 263–268, 1996.
- 669 [26] D. Stark, "The moisture condition of field concrete exhibiting alkali-silica reactivity,"  
670 in *Durability of concrete. G. M. IDORN International Symposium*, 1992, pp. 973–987.
- 671 [27] J. Verdier, "Contribution à la caractérisation de l'évolution du taux de fuite des enceintes  
672 de confinement du parc nucléaire," PhD Thesis, Université Paul Sabatier, Toulouse, France,  
673 2001.
- 674 [28] L. Granger, "Comportement différé du béton dans les enceintes de centrales nucléaires:  
675 analyse et modélisation," PhD Thesis, Ecole Nationale des Ponts et Chaussées, Marne-La-  
676 Vallée, France, 1996.

- 677 [29] S. Goto, D.M. Roy, “The effect of W/C ratio and curing temperature on the permeability  
678 of hardened cement paste,” *Cem. Concr. Res.*, vol. 11, pp. 575–579, 1981.
- 679 [30] M. Jooss, H.W. Reinhardt, “Permeability and diffusivity of concrete as function of  
680 temperature,” *Cem. Concr. Res.*, vol. 32, pp. 1497–1504, 2002.
- 681 [31] M. Choinska, A. Khelidj, G. Chatzigeorgiou, and G. Pijaudier-Cabot, “Effects and  
682 interactions of temperature and stress-level related damage on permeability of concrete,” *Cem.*  
683 *Concr. Res.*, vol. 37, no. 1, pp. 79–88, 2007.
- 684 [32] A.N. Noumowe, R. Siddique, G. Debicki, “Permeability of high-performance concrete  
685 subjected to elevated temperature (600 °C),” *Constr. Build. Mater.*, vol. 23, pp. 1855–1861,  
686 2009.
- 687 [33] F. Jacobs, “Permeability to gas of partially saturated concrete,” *Mag. Conc. Res.*, vol.  
688 50, pp. 115-121, 1998.
- 689 [34] A. Abbas, M. Carcasses, and J.-P. Ollivier, “Gas permeability of concrete in relation to  
690 its degree of saturation,” *Mater. Struct.*, vol. 32, no. 1, pp. 3–8, 1999.
- 691 [35] Z. A. Kameche, F. Ghomari, M. Choinska, and A. Khelidj, “Assessment of liquid water  
692 and gas permeabilities of partially saturated ordinary concrete,” *Constr. Build. Mater.*, vol. 65,  
693 pp. 551–565, 2014.
- 694 [36] H. Kallel, “Effet du degré de saturation et de la température sur le comportement  
695 mécanique du béton,” in *13ème Journées d’études des Milieux Poreux*, 2016.
- 696 [37] E. Oukhemanou, S. Desforges, E. Buchoud, S. Michel-Ponnelle, A. Courtois,  
697 “VeRCoRs Mock-Up: Comprehensive Monitoring System for Reduced Scale Containment  
698 Model,” *Technological Innovations in Nuclear Civil Engineering TINCE*, 2016, Paris, France.
- 699 [38] H. E. A. Sogbossi, “Etude de l’évolution de la perméabilité du béton en fonction de son  
700 endommagement : transposition des résultats de laboratoire à la prédiction des débits de fuite  
701 sur site,” Ph.D. Thesis, Université de Toulouse, Université Toulouse III - Paul Sabatier, 2017.
- 702 [39] V. Waller, “Relations entre composition des betons, exothermie en cours de prise et  
703 resistance en compression,” ENPC, 1999.
- 704 [40] C. Antón, M. A. Climent, G. de Vera, I. Sánchez, and C. Andrade, “An improved  
705 procedure for obtaining and maintaining well characterized partial water saturation states on  
706 concrete samples to be used for mass transport tests,” *Mater. Struct.*, vol. 46, no. 8, pp. 1389–  
707 1400, 2012.
- 708 [41] RILEM TC 116-PCD, “Permeability of concrete as a criterion of its durability, final  
709 report,” *Mater. Struct.*, vol. 32, no. 217, pp. 163–173, 1999.
- 710 [42] M. Carcassès, A. Abbas, J.-P. Ollivier, and J. Verdier, “An optimised preconditioning  
711 procedure for gas permeability measurement,” *Mater. Struct.*, vol. 35, no. 1, pp. 22–27, 2002.
- 712 [43] Z. Wu, H.S. Wong, N.R. Buenfeld, “Influence of drying-induced microcracking and  
713 related size effects on mass transport properties of concrete,” *Cem. Concr. Res.*, vol. 68, pp.  
714 35–48, 2015.
- 715 [44] NF EN 12390-3, “Essais pour béton durci - Partie 3 : résistance à la compression des  
716 éprouvettes,” AFNOR, 2003.
- 717 [45] RILEM TC, RILEM Recommendations for the Testing and Use of Constructions  
718 Materials - CPC 8 Modulus of elasticity of concrete in compression, 1994.

- 719 [46] J. J. Kollek, "The determination of the permeability of concrete to oxygen by the  
720 Cembureau method-a recommendation," *Mater. Struct.*, vol. 22, no. 3, pp. 225–230, 1989.
- 721 [47] Norme XP P18-463, Norme XP P18-463 - Essai pour béton durci - Essai de perméabilité  
722 à l'air. 1999.
- 723 [48] V. Garnier, C. Payan, L. Martin et al., "Non-destructive evaluation of containment walls  
724 in nuclear power plants," 43rd annual review of progress in quantitative nondestructive  
725 evaluation, Vol. 36, AIP Conference Proceedings, 1806(1):080018, 2017.
- 726 [49] B. Masson, "Démarche industrielle de compréhension des phénomènes de transferts  
727 dans les parois en béton," 31èmes Rencontres de l'AUGC, ENS Cachan, 2013.
- 728 [50] S. Medjigbodo, A. Darquennes, C. Aubernon, A. Loukili, "Effects of the air – steam  
729 mixture on the permeability of damaged concrete," *Cem. Concr. Res.*, vol. 54, pp. 98–105,  
730 2013.
- 731 [51] S. Pihlajavaara, "A review of some of the main results of a research on the ageing  
732 phenomena of concrete: effect of moisture conditions on strength, shrinkage and creep of  
733 mature concrete," *Cem. Concr. Res.*, vol. 4, pp. 761–771, 1974.
- 734 [52] V. Kanna, O. RA, J. HM, "Effect of shrinkage and moisture content on the physical  
735 characteristics of blended cement mortars," *Cem. Concr. Res.*, vol. 28, pp. 1467–1477, 1998.
- 736 [53] I. Yaman, N. Hearn, H. Aktan, "Active and non-active porosity in concrete Part I:  
737 Experimental evidence," *Mater. Struct.*, vol. 35, pp. 102–109, 2002.
- 738 [54] I. Yurtdas, N. Burlion, and F. Skoczylas, "Triaxial mechanical behaviour of mortar:  
739 Effects of drying," *Cem. Concr. Res.*, vol. 34, no. 7, pp. 1131–1143, 2004.
- 740 [55] N. Burlion, F. Bourgeois, J. Shao, "Effects of desiccation on mechanical behaviour of  
741 concrete," *Cem. Concr. Compos.*, vol. 27, pp. 367–379, 2005.
- 742 [56] G. Villain, L. Le Marrec, and L. Rakotomanana, "Determination of the bulk elastic  
743 moduli of various concretes by resonance frequency analysis of slabs submitted to impact  
744 echo," *Eur. J. Environ. Civ. Eng.*, vol. 15, no. 4, pp. 601–617, 2011.
- 745 [57] I. Maruyama, H. Sasano, Y. Nishioka, G. Igarashi, "Strength and Young's modulus  
746 change in concrete due to long-term drying and heating up to 90 °C," *Cem. Concr. Res.*, vol.  
747 66, pp. 48–63, 2014.
- 748 [58] W. Wang, C. Lu, G. Yuan, Y. Zhang, "Effects of pore water saturation on the  
749 mechanical properties of fly ash concrete," *Constr. Build. Mater.*, vol. 130, pp. 54–63, 2017.
- 750 [59] I. Yurtdas, N. Burlion, J.-F. Shao, and A. Li, "Evolution of the mechanical behaviour of  
751 a high performance self-compacting concrete under drying," *Cem. Concr. Compos.*, vol. 33,  
752 no. 3, pp. 380–388, 2011.
- 753 [60] H. Sogbossi, J. Verdier, and S. Multon, "Impact of reinforcement-concrete interfaces  
754 and cracking on gas transfer in concrete," *Constr. Build. Mater.*, vol. 157, pp. 521–533, 2017.
- 755 [61] G. Torelli, P. Mandal, M. Gillie, and V.-X. Tran, "Concrete strains under transient  
756 thermal conditions: A state-of-the-art review," *Eng. Struct.*, vol. 127, pp. 172–188, 2016.
- 757 [62] K. Li, M. Stroeven, P. Stroeven, L. J. Sluys, "Effects of technological parameters on  
758 permeability estimation of partially saturated cement paste by a DEM approach, *Cem. Concr.*  
759 *Compos.*, vol. 84, pp. 222–231, 2017.

- 760 [63] J. Verdier and M. Carcassès, “Equivalent gas permeability of concrete samples  
761 subjected to drying,” *Mag. Concr. Res.*, vol. 56, no. 4, pp. 223–230, 2004.
- 762 [64] M. T. V. Genuchten, “A Closed-form Equation for Predicting the Hydraulic  
763 Conductivity of Unsaturated Soils 1,” *Soil Sci. Soc. Am. J.*, vol. 44, no. 5, pp. 892–898, 10/01  
764 1980.
- 765 [65] L. Jason, “Relation endommagement perméabilité pour les bétons : application aux  
766 calculs de structures,” PhD Thesis, Université de Nantes, 2004.
- 767 [66] V. Baroghel-Bouny, “Caractérisation microstructurale et hydrique des pâtes de ciment  
768 et des bétons ordinaires et à très hautes performances,” Ph.D. Thesis, Ecole Nationale des Ponts  
769 et Chaussées, 1994.
- 770 [67] J. P. Monlouis-Bonnaire, J. Verdier, and B. Perrin, “Prediction of the relative  
771 permeability to gas flow of cement-based materials,” *Cem. Concr. Res.*, vol. 34, no. 5, pp. 737–  
772 744, 2004.
- 773 [68] M. Choinska, “Effets de la température, du chargement mécanique et de leurs  
774 interactions sur la perméabilité du béton de structure,” PhD Thesis, Ecole Centrale de Nantes;  
775 Université de Nantes, 2006.
- 776 [69] F. Ghasemzadeh, R. Rashednia, D. Smyl, M. Pour-Ghaz, “A comparison of methods to  
777 evaluate mass transport in damaged mortar”, *Cem. Concr. Compos.*, vol. 70, pp. 119–129, 2016.
- 778 [70] V. Picandet, “Influence d’un endommagement mécanique sur la perméabilité et sur la  
779 diffusivité hydrique des bétons,” PhD Thesis, Ecole Centrale de Nantes, 2001.
- 780 [71] R. Bucher, T. Vidal, A. Sellier, and J. Verdier, “Effet du séchage sur les propriétés  
781 mécaniques des matériaux cimentaires,” in 23ème Congrès Français de Mécanique, 2017.
- 782 [72] X. H. Vu, ‘Caractérisation expérimentale du béton sous fort confinement : influences du  
783 degré de saturation et du rapport eau/ciment’, PhD Thesis, Université Joseph-Fourier-Grenoble  
784 I, 2007.
- 785 [73] P. Chhun, “Modélisation du comportement thermo-hydro-chemo-mécanique des  
786 enceintes de confinement nucléaire en béton armé-précontraint,” PhD Thesis, Université  
787 Toulouse III-Paul Sabatier, 2017.
- 788 [74] U. Schneider, “Concrete at high temperatures — A general review,” *Fire Saf. J.*, vol.  
789 13, no. 1, pp. 55–68, 1988.
- 790 [75] Z. P. Bažant and W. Thonguthai, “Pore Pressure and Drying of Concrete at High  
791 Temperature,” *J. Eng. Mech. Div.*, vol. 104, no. 5, pp. 1059–1079, 1978.
- 792 [76] S. Rahal, A. Sellier, G. Casaux-Ginestet, “Finite Element Modelling of permeability in  
793 brittle materials cracked in tension,” *Int. J. Solids Struct.*, vol. 113–114, pp. 85–99, 2017.
- 794 [77] V. Picandet, A. Khelidj, and G. Bastian, “Effect of axial compressive damage on gas  
795 permeability of ordinary and high-performance concrete,” *Cem. Concr. Res.*, vol. 31, no. 11,  
796 pp. 1525–1532, 2001.
- 797 [78] M. Hoseini, V. Bindiganavile, N. Banthia, “The effect of mechanical stress on  
798 permeability of concrete: A review”, *Cem. Concr. Compos.*, vol. 31, pp. 213–220, 2009
- 799 [79] S. Rahal, A. Sellier, and J. Verdier, “Modelling of change in permeability induced by  
800 dilatancy for brittle geomaterials,” *Constr. Build. Mater.*, vol. 125, pp. 613–624, 2016.